Eur. Phys. J. D **40**, 91–99 (2006)
DOI: 10.1140/epjd/e2006-00139-6

THE EUROPEAN PHYSICAL JOURNAL D

Radiative lifetime and oscillator strength determinations in potassium ions (K V, K VI and K VII)

É. Biémont[1,2,a], H.-P. Garnir[1], P.-H. Lefèbvre[1], P. Palmeri[2], L. Philippart[2], P. Quinet[1,2], D. Rostohar[1], and C.J. Zeippen[3]

[1] Institut de Physique Nucléaire, Atomique et de Spectroscopie, Université de Liège, Sart Tilman (Bât. B15), B-4000 Liège, Belgium
[2] Astrophysique et Spectroscopie, Université de Mons-Hainaut, B-7000 Mons, Belgium
[3] UMR 8102 (associée au CNRS et à l'Université Paris-7) et LUTh, Observatoire de Paris, F-92195 Meudon, France

Received 17 February 2006 / Received in final form 12 April 2006
Published online 15 June 2006 –

Abstract. Oscillator strengths have been calculated for the transitions depopulating levels of the $3s^2 3p^3$, $3s3p^4$ configurations of K V, of the $3s^2 3p^2$, $3s3p^3$ configurations of K VI and of the $3s^2 3p$, $3s3p^2$, $3p^3$ and $3s3p3d$ configurations of K VII. A multiconfiguration Dirac-Fock method, incorporating the relativistic two-body Breit interaction and quantum electrodynamics corrections due to self-energy and vacuum polarization, has been used for the calculations. The reliability of this approach has been tested by comparison with relativistic Hartree-Fock calculations and also with some experimental measurements performed by beam-foil spectroscopy at a beam energy of 1.7 MeV.

PACS. 32.70.Cs Oscillator strengths, lifetimes, transition moments – 32.30.-r Atomic spectra – 31.25.-v Electron correlation calculations for atoms and molecules

1 Introduction

Radiative parameters in moderately charged ions are useful and needed for diagnostics of astrophysical and laboratory plasmas. Transition probabilities in potassium ions (K V, K VI and K VII) are still very sparse. In K V, the only experimental data have been obtained by beam-foil spectroscopy [1] more than 30 years ago. On the theoretical side, a limited number of oscillator strengths have been published in the same ion both for allowed [2–9] or for forbidden transitions [10,11] (M1 or E2 transitions).

In K VI so far, there are no experimental transition probabilities or lifetimes available. Attempts to provide theoretical oscillator strengths for E1 transitions are due to several authors [2,12–20] who used different theoretical approaches. Radiative parameters have also been reported for forbidden (E2 and M1) transitions by Mendoza and Zeippen [21] and Biémont and Bromage [22].

The only experimental data published for K VII (aluminium isoelectronic sequence) are due to Engström et al. [23]. Theoretical lifetimes and transition probabilities, however, have been reported for allowed transitions along the sequence [2,13,24–35]. A number of data are also available for forbidden transitions [36,37].

Some of the available theoretical data were published a long time ago when the computer power was still very limited. Additional calculations (see e.g. [6,7,9,16,18,20,30]) were devoted to the aluminium, silicon or phosphorus sequences in general and were not focussing specially on the potassium ions. Consequently, the models adopted for the ions along the sequences take configuration interactions into account in a uniform way, the authors being more interested in the trends of results along the sequences than in the individual transition probabilities for a specific ion.

The purpose of the present work is to provide some refined data (lifetimes and oscillator strengths) for selected transitions of K V, K VI and K VII. A multiconfiguration Dirac-Fock method (MCDF) approximation, incorporating the relativistic two-body Breit interaction and quantum electrodynamics corrections (QED) due to self-energy and vacuum polarization, has been used for the calculations. The accuracy of the calculations is assessed through a comparison of the MCDF results with those obtained with a Relativistic Hartree-Fock (HFR) approximation and with selected experimental measurements performed with the beam-foil spectroscopy (BFS). This technique remains one of the rare methods susceptible to produce potassium ions in the intermediate ionization degrees considered in the present paper.

2 Calculations

2.1 The MCDF method and results

A well-known fully relativistic approach which does provide accurate atomic data in many different situations is

[a] e-mail: E.Biemont@ulg.ac.be

the MCDF method which is based on the Dirac equation. The code used, GRASP92 [38], is a recent version of the General-purpose Relativistic Atomic Structure Program (GRASP) initially written by Grant and coworkers [39–41]. GRASP92 uses sparse-matrix representation and dynamic allocation techniques to improve the treatment of large dimension Hamiltonian matrices [38]. It has been used with success for computing oscillator strengths in heavy ions like Tl II and Tl III [42], Hg II [43] and, more recently, Cd-like ions [44] and Bi II [45]. This code is based on the MCDF approach in which the atomic state functions (ASF), $\Psi(\gamma JM_J)$, are expanded in linear combinations of configuration state functions (CSF), $\Phi(\alpha_i JM_J)$, according to

$$\Psi(\gamma JM_J) = \sum_i c_i \Phi(\alpha_i JM_J). \quad (1)$$

The CSF are in turn linear combinations of Slater determinants constructed from monoelectronic spin-orbitals of the form:

$$u_{n\kappa m}(r,\theta,\phi) = \frac{1}{r}\begin{pmatrix} P_{n\kappa}(r)\chi_{\kappa m}(\theta,\phi) \\ iQ_{n\kappa}(r)\chi_{-\kappa m}(\theta,\phi)\end{pmatrix} \quad (2)$$

where $P_{n\kappa}(r)$ and $Q_{n\kappa}(r)$ are, respectively, the large and small component radial wave functions, and the angular functions $\chi_{\kappa m}(\theta,\phi)$ are the spinor spherical harmonics [39]. The α_i represent all the one-electron and intermediate quantum numbers needed to completely define the CSF. γ is usually chosen as the α_i corresponding to the CSF with the largest weight $|c_i|^2$. The quantum number κ is given by $\kappa = \pm(j+1/2)$ where j is the electron total kinetic moment. The radial functions $P_{n\kappa}(r)$ and $Q_{n\kappa}(r)$ are numerically represented on a logarithmic grid and are required to be orthonormal within each κ symmetry. In the MCDF variational procedure, the radial functions and the expansion coefficients c_i are optimized to self-consistency.

In the three ions (K V, K VI and K VII), we did consider the active space (AS) method for building the MCDF multiconfiguration expansion. The latter is produced by exciting the electrons from the reference configurations to a given set of orbitals. The rules adopted for generating the configuration space differ according to the correlation model being used. Within a given correlation model, the AS of orbitals spanning the configuration space is increased to monitor the convergence of the total energies and the oscillator strengths.

The QED effects were found to be small: in fact, the correction to the energy levels was reaching a few (<5 cm^{-1}) for the ground configurations in the three ions and a few tens (<80) of cm^{-1} for the $3s3p^4$, $3s3p^3$, $3s3p^2$ configurations in K V, K VI and K VII, respectively. The largest correction was reaching 160 cm^{-1} for the $3p^3$ configuration of K VII.

2.1.1 K V

The MCDF calculations have been dedicated to the levels of K V below 200 000 cm^{-1} for which the lifetimes have been measured by BFS (see further). They have been carried out in 3 steps. An energy functional has been built from the 12 lowest ASF using the Extended Optimal Level (EOL) option and the configurations $3s^23p^3$ $J = 1/2$–$5/2$ and $3s3p^4$ $J = 1/2$–$5/2$ have been used as references along all the calculation steps. In the first step, the core orbitals, i.e. $1s$ to $2p$, together with the orbitals $3s$ and $3p$, have been optimized. The 13 CSF belonging to the reference configurations have been exclusively considered in the configuration space. The second step has consisted in increasing to 752 CSF the configuration space by considering up to quadruple virtual electron excitations to the $\{3s, 3p, 3d\}$ orbital set. In the third step, the configuration space has been extended further to 4477 CSF by adding the single and double excitations to the $n = 4$ orbitals. Only the newly introduced orbitals have been optimized in the last two steps. We have not managed to include virtual excitations to the 5λ ($n\lambda$ stands for nl and nl_-) orbitals because of memory limitations.

A comparison between the calculated and the experimental low-lying energy levels is given in Table 1. The MCDF lifetimes are presented in Table 2 (column 6) where they are compared with the HFR results (column 7) (see Sect. 2.2) and with the experimental results when they are available.

In Table 3, we report the MCDF oscillator strengths corrected with the experimental wavelengths for transitions depopulating the levels tabulated in Table 1. The Babushkin and the Coulomb gauges results are both reported in Tables 2 and 3, an agreement between the two formalisms being a necessary but not a sufficient condition for the accuracy of the results.

2.1.2 K VI

In the present study, we have focused our calculations in K VI on the determination of the oscillator strengths of the transitions originating from the level $3s3p^3\ {}^1P_1^\circ$ for which a lifetime has been obtained by BFS in the present work (see further) and from the other $J = 1$ levels in the same configuration. In order to do so, we have proceeded in four steps. In all the steps, the configuration spaces have been built from the reference configurations $3s^23p^2$ $J = 0$–2 and $3s3p^3$ $J = 1$, and the energy functional used in the variational procedure was based on the lowest 9 ASF within the framework of EOL option [38]. The first step has consisted in optimizing the core orbitals, i.e. $1s$ to $2p$, together with the orbitals $3s$ and $3p$. The AS contained the 9 CSF belonging to the reference configurations and so no correlation has been considered here. In the following steps, the AS has been increased to 142, 1377 and 4616 CSF by considering all the single and double virtual electron excitations to the $\{3s, 3p, 3d\}$, $\{3s, 3p, 3d, 4s, 4p, 4d, 4f\}$ and $\{3s, 3p, 3d, 4s, 4p, 4d, 4f, 5s, 5p, 5d, 5f, 5g\}$ orbital sets, respectively. In each step, the newly introduced orbitals have been optimized fixing those included in the preceding steps.

In Table 1, a comparison between the MCDF eigenvalues issued from the last step of the calculations and

Table 1. Comparison between experimental and MCDF energy levels in K V, K VI and K VII.

Ion	Design.[a]	J	E^a_{Expt} (cm^{-1})	E^b_{MCDF} (cm^{-1})	Δ^c (cm^{-1})
K V	$3s^2 3p^3\ ^4S^\circ$	3/2	0.0	0	0
	$3s^2 3p^3\ ^2D^\circ$	3/2	24012.5	25230	–1218
		5/2	24249.6	25458	–1208
	$3s^2 3p^3\ ^2P^\circ$	1/2	39758.1	41275	–1517
		3/2	40080.2	41579	–1499
	$3s3p^4\ ^4P$	5/2	136636.5	137548	–912
		3/2	138037.5	138936	–899
		1/2	138804.1	139698	–894
	$3s3p^4\ ^2D$	3/2	169579.5	172551	–2972
		5/2	169705.8	172677	–2971
	$3s3p^4\ ^2P$	3/2	194805.1	200557	–5752
		1/2	196331.2	202076	–5745
K VI	$3s^2 3p^2\ ^3P$	0	0.0	0	0
		1	1133.4	1117	16
		2	2927.2	2898	29
	$3s^2 3p^2\ ^1D$	2	18977.8	19319	–341
	$3s^2 3p^2\ ^1S$	0	43358.8	43900	–541
	$3s3p^3\ ^3D^\circ$	1	140741.3	141208	–467
	$3s3p^3\ ^3P^\circ$	1	163435.0	164340	–905
	$3s3p^3\ ^3S^\circ$	1	218317.3	222711	–4394
	$3s3p^3\ ^1P^\circ$	1	223840.1	229266	–5426
K VII	$3s^2 3p\ ^2P^\circ$	1/2	0.0	0	0
		3/2	3134.0	3075	59
	$3s3p^2\ ^4P$	1/2	114650 + x	113842	808
		3/2	115786 + x	114956	830
		5/2	117523 + x	116677	846
	$3s3p^2\ ^2D$	3/2	151883.9	151663	221
		5/2	152051.7	151835	217
	$3s3p^2\ ^2S$	1/2	193084.5	194518	–1434
	$3s3p^2\ ^2P$	1/2	206502.9	209806	–3303
		3/2	208432.5	211452	–3020
	$3s^2 3d\ ^2D$	3/2	250663	252808	–2145
		5/2	250781	252910	–2129
	$3p^3\ ^4S^\circ$	3/2	307777 + x	309847	–2070
	$3s3p3d\ ^4P^\circ$	5/2	362492 + x	363226	–734
		3/2	363321 + x	364071	–750
	$3s3p3d\ ^4D^\circ$	1/2	365688 + x	367068	–1380
		3/2	366101 + x	367227	–1126
		5/2	366409 + x	367551	–1142
		7/2	366556 + x	367717	–1161

[a] NIST database [46]. x in column 4 means that the NIST energy levels are not accurately determined. [b] Step 3 of the MCDF calculation for K V, step 4 of the MCDF calculation for K VI and K VII (see the text). [c] $E_{Expt} - E_{MCDF}$.

the experimental energy levels, as tabulated in the NIST database [46], is presented. The MCDF lifetimes obtained in this work are shown in Table 2 and the corresponding oscillator strengths, restricted to the transitions with $\log gf > -3.00$, are reported in Table 4.

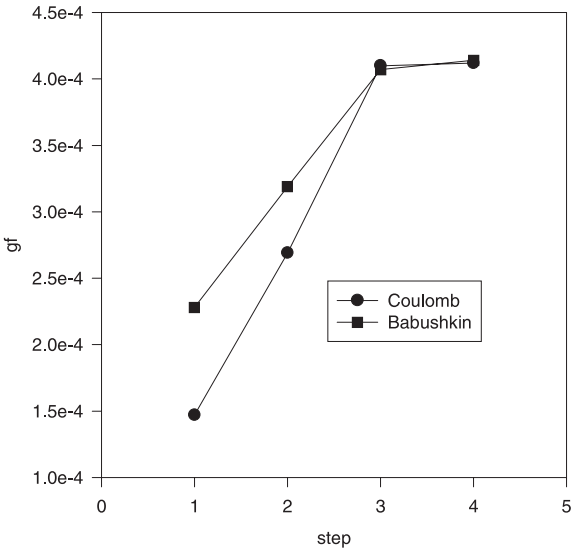

Fig. 1. Convergence of the weighted oscillator strength of the intersystem transition $3s^2 3p\ ^2P^\circ_{3/2} - 3s3p^2\ ^4P_{5/2}$ of K VII. The results have been calculated in the two formalisms.

2.1.3 K VII

In the present work, we have focused on the radiative properties of the first levels of K VII, i.e. the levels with energies less than 370 000 cm^{-1} (see the NIST database). For doing so, we have proceeded in four steps. In the first one, an active space have been generated by considering all the 33 CSF belonging to the configurations $3s^2 3p$ $J = 1/2$, 3/2, $3s3p^2$ $J = 1/2$–5/2, $3s^2 3d$ $J = 3/2$, 5/2, $3p^3$ $J = 3/2$ and $3s3p3d$ $J = 1/2$–7/2. The core orbitals, i.e. $1s$ to $2p$, together with all the orbitals with a principal quantum number, n, equal to 3 have been optimized minimizing an energy functional built from the above mentioned 33 CSF using the EOL option [38]. The AS has been increased to 119 CSF in the second step by adding CSF generated by single and double electron excitations within the $n = 3$ orbitals starting from the reference configurations used in the first step. 3λ orbitals have been optimized minimizing the same functional as in the previous step, the core orbitals being kept fixed. The third step consisted in extending the AS to 1409 CSF by considering all the single and double excitations to the $\{3s, 3p, 3d, 4s, 4p, 4d, 4f\}$ orbital set. The newly included orbitals, i.e. $n = 4$ orbitals, were optimized fixing the others. In the fourth step, the 5λ orbitals have been included and optimized in the same way as in the previous step. The AS has been increased to 5254 CSF.

In Figure 1, we monitor the convergence of the weighted oscillator strength of the intersystem transition $3s^2 3p\ ^2P_{3/2} - 3s3p^2\ ^4P^\circ_{5/2}$. A good agreement between the two gauges (Coulomb and Babushkin) can be seen in the last two steps.

We present in Table 1 a comparison between the MCDF eigenvalues and the experimental energy levels tabulated in the NIST database [46]. In the last column, the differences between these two sets of values are displayed. The quasi-constant deviations, within each

Table 2. Comparison between experimental, MCDF and HFR lifetimes in K V, K VI and K VII.

Ion	Level[a]	Energy[a] (cm^{-1})	λ_{obs} (nm)	Lifetime (ns) Expt.	MCDF[d]	HFR
K V	$3s3p^4\ ^4P_{5/2}$	136636.5	73.2	2.80 ± 0.09^{be} 2.9 ± 0.2^{c}	2.47/2.23	2.02
	$3s3p^4\ ^4P_{3/2}$	138037.5	72.4	2.44 ± 0.25^{be} 2.9 ± 0.2^{c}	2.41/2.18	1.98
	$3s3p^4\ ^4P_{1/2}$	138804.1			2.37/2.14	1.95
	$3s3p^4\ ^2D_{3/2}$	169579.5			1.20/1.12	0.92
	$3s3p^4\ ^2D_{5/2}$	169705.8	68.7	1.8 ± 0.5^{bf}	1.24/1.15	0.94
	$3s3p^4\ ^2P_{3/2}$	194805.1	58.6	0.80 ± 0.05^{bf}	0.47/0.47	0.75
	$3s3p^4\ ^2P_{1/2}$	196331.2	58.0	0.79 ± 0.05^{bf}	0.46/0.46	0.70
K VI	$3s3p^3\ ^3D^\circ_1$	140741.3			2.37/2.31	2.80
	$3s3p^3\ ^3P^\circ_1$	163435.0			0.79/0.78	0.97
	$3s3p^3\ ^3S^\circ_1$	218317.3			0.039/0.039	0.042
	$3s3p^3\ ^1P^\circ_1$	223840.1	48.8	0.092 ± 0.005^{be}	0.069/0.070	0.064
K VII	$3s3p^2\ ^4P_{1/2}$	$114650 + x$			924/851	836
	$3s3p^2\ ^4P_{3/2}$	$115786 + x$			4677/4482	3786
	$3s3p^2\ ^4P_{5/2}$	$117523 + x$			1650/1656	1430
	$3s3p^2\ ^2D_{3/2}$	151883.9	65.8	1.8 ± 0.4^{bf}	1.55/1.62	1.52
	$3s3p^2\ ^2D_{5/2}$	152051.7	67.1	1.9 ± 0.3^{bf}	1.66/1.73	1.61
	$3s3p^2\ ^2S_{1/2}$	193084.5	52.6	0.12 ± 0.01^{bfe}	0.168/0.165	0.176
	$3s3p^2\ ^2P_{1/2}$	206502.9			0.059/0.059	0.061
	$3s3p^2\ ^2P_{3/2}$	208432.5			0.058/0.058	0.060
	$3s^23d\ ^2D_{3/2}$	250663			0.047/0.046	0.048
	$3s^23d\ ^2D_{5/2}$	250781			0.049/0.047	0.050
	$3p^3\ ^4S^\circ_{3/2}$	$307777 + x$			0.066/0.065	0.069
	$3s3p3d\ ^4P^\circ_{5/2}$	$362492 + x$			0.079/0.076	0.079
	$3s3p3d\ ^4P^\circ_{3/2}$	$363321 + x$	40.4	0.06 ± 0.01^{be}	0.076/0.073	0.075
	$3s3p3d\ ^4D^\circ_{1/2}$	$365688 + x$			0.048/0.046	0.049
	$3s3p3d\ ^4D^\circ_{3/2}$	$366101 + x$			0.049/0.047	0.050
	$3s3p3d\ ^4D^\circ_{5/2}$	$366409 + x$			0.048/0.046	0.049
	$3s3p3d\ ^4D^\circ_{7/2}$	$366556 + x$			0.047/0.046	0.048

[a] NIST database [46]. x in column 3 means that the NIST energy levels are not accurately known. [b] BFS (this work). [c] BFS [1]. [d] Step 3 (see the text) of the MCDF calculation for K V, step 4 for K VI and K VII. Babushkin/Coulomb gauges. The quoted values have been corrected with the experimental wavelengths. [e] Channeltron detector used for the measurements. [f] CCD detector used for the measurements.

spectroscopic term, show a good restitution of the fine structure if we except the levels $3s3p^2\ ^2P_{1/2}$ and $3s3p3d\ ^4D^\circ_{1/2}$ which are strongly perturbed by neighbouring states.

The MCDF lifetimes obtained in this study are shown in Table 2. The theoretical values are calculated from MCDF transition probabilities corrected by incorporating the experimental energies. An overall agreement is found between the two gauges indicating the good quality of the MCDF calculation.

In Table 5, we report the MCDF oscillator strengths corrected with the experimental wavelengths for transitions depopulating the levels tabulated in Table 1. The Babushkin and the Coulomb values are presented to give a more precise idea of the quality of the data.

2.2 The HFR approach and the corresponding results

In order to assess the reliability of the MCDF calculations, the results have been compared with those obtained with a completely independent theoretical method i.e. the HFR approach. Although based on the Schrödinger equation, this approach takes the most important relativistic effects (mass and velocity effects, Darwin correction) into account. In addition, configuration interaction can be considered in the calculations in a very flexible way.

Concretely, in the present work, HFR calculations have been performed for the three ions considered using the suite of computer codes of Cowan [47] in which we have incorporated the core-polarization effects (HFR + CP approach) (For a detailed description, see e.g. [48]).

Table 3. Oscillator strengths for transitions depopulating the levels of the configuration $3s3p^4$ in K V. The table has been restricted to transitions with log $gf > -3.00$.

Transition[a]	λ^b (nm)	log gf^c
$3s3p^4\ ^4P_{5/2} - 3s^23p^3\ ^4S^\circ_{3/2}$	73.187	–0.71/–0.67
$3s3p^4\ ^4P_{3/2} - 3s^23p^3\ ^4S^\circ_{3/2}$	72.444	–0.88/–0.84
$3s3p^4\ ^4P_{1/2} - 3s^23p^3\ ^4S^\circ_{3/2}$	72.044	–1.18/–1.14
$3s3p^4\ ^2D_{3/2} - 3s^23p^3\ ^2D^\circ_{3/2}$	68.697	–0.70/–0.67
$3s3p^4\ ^2D_{3/2} - 3s^23p^3\ ^2D^\circ_{5/2}$	68.809	–1.85/–1.81
$3s3p^4\ ^2D_{3/2} - 3s^23p^3\ ^2P^\circ_{1/2}$	77.029	–1.61/–1.59
$3s3p^4\ ^2D_{3/2} - 3s^23p^3\ ^2P^\circ_{3/2}$	77.220	–3.01/–2.97
$3s3p^4\ ^2D_{5/2} - 3s^23p^3\ ^2D^\circ_{3/2}$	68.637	–1.87/–1.84
$3s3p^4\ ^2D_{5/2} - 3s^23p^3\ ^2D^\circ_{5/2}$	68.749	–0.54/–0.51
$3s3p^4\ ^2D_{5/2} - 3s^23p^3\ ^2P^\circ_{3/2}$	77.145	–1.28/–1.25
$3s3p^4\ ^2P_{3/2} - 3s^23p^3\ ^2D^\circ_{3/2}$	58.551	–1.39/–1.40
$3s3p^4\ ^2P_{3/2} - 3s^23p^3\ ^2D^\circ_{5/2}$	58.632	–0.46/–0.46
$3s3p^4\ ^2P_{3/2} - 3s^23p^3\ ^2P^\circ_{1/2}$	64.497	–1.91/–1.86
$3s3p^4\ ^2P_{3/2} - 3s^23p^3\ ^2P^\circ_{3/2}$	64.631	–1.36/–1.31
$3s3p^4\ ^2P_{1/2} - 3s^23p^3\ ^2D^\circ_{3/2}$	58.032	–0.74/–0.75
$3s3p^4\ ^2P_{1/2} - 3s^23p^3\ ^2P^\circ_{1/2}$	63.868	–1.48/–1.43
$3s3p^4\ ^2P_{1/2} - 3s^23p^3\ ^2P^\circ_{3/2}$	64.000	–2.00/–1.97

[a] Designation of the levels according to the NIST database [46]. The transitions are given in emission. [b] Calculated from the experimental energy levels given in the NIST database [46]. [c] Step 3 of the MCDF calculation (see the text). The values have been corrected for the experimental wavelengths. Babushkin/Coulomb gauges.

Table 4. Oscillator strengths for transitions depopulating the levels of the configuration $3s3p^3$ in K VI. The table has been restricted to transitions with log $gf > -3.00$.

Transition[a]	λ^b (nm)	log gf^c
$3s3p^3\ ^3D^\circ_1 - 3s^23p^2\ ^3P_0$	71.052	–1.22/–1.21
$3s3p^3\ ^3D^\circ_1 - 3s^23p^2\ ^3P_1$	71.629	–1.46/–1.45
$3s3p^3\ ^3D^\circ_1 - 3s^23p^2\ ^3P_2$	72.562	–2.83/–2.81
$3s3p^3\ ^3P^\circ_1 - 3s^23p^2\ ^3P_0$	61.186	–1.15/–1.15
$3s3p^3\ ^3P^\circ_1 - 3s^23p^2\ ^3P_1$	61.614	–1.18/–1.17
$3s3p^3\ ^3P^\circ_1 - 3s^23p^2\ ^3P_2$	62.302	–1.10/–1.09
$3s3p^3\ ^3S^\circ_1 - 3s^23p^2\ ^3P_0$	45.805	–0.56/–0.56
$3s3p^3\ ^3P^\circ_1 - 3s^23p^2\ ^3P_1$	46.044	–0.09/–0.10
$3s3p^3\ ^3P^\circ_1 - 3s^23p^2\ ^3P_2$	46.427	0.14/0.13
$3s3p^3\ ^3P^\circ_1 - 3s^23p^2\ ^1D_2$	50.166	–1.52/–1.54
$3s3p^3\ ^3P^\circ_1 - 3s^23p^2\ ^1S_0$	57.156	–2.15/–2.10
$3s3p^3\ ^1P^\circ_1 - 3s^23p^2\ ^3P_0$	44.675	–1.99/–2.02
$3s3p^3\ ^1P^\circ_1 - 3s^23p^2\ ^3P_1$	44.902	–1.31/–1.32
$3s3p^3\ ^1P^\circ_1 - 3s^23p^2\ ^3P_2$	45.267	–1.49/–1.49
$3s3p^3\ ^1P^\circ_1 - 3s^23p^2\ ^1D_2$	48.813	0.11/0.10
$3s3p^3\ ^1P^\circ_1 - 3s^23p^2\ ^1S_0$	55.407	–0.68/–0.64

[a] Designation of the levels according to the NIST database [46]. The transitions are given in emission. [b] Calculated from the experimental energy levels given in the NIST database [46]. [c] Step 4 of the MCDF calculation (see the text). Corrected for the experimental wavelengths. Babushkin/Coulomb gauges.

2.2.1 HFR calculations in K V

For the K V ion, the configurations explicitly retained in the calculations were $3s^23p^3$, $3s^23p^24p$, $3s^23p^24f$, $3p^33d^2$, $3s3p^3nd$ ($n = 3, 4$), $3s3p^34s$, $3s3p^23d4p$, $3s3p^23d4f$, $3p^5$, $3p^44p$, $3p^44f$, $3p^33d^2$, $3p^33d4d$, $3p^33d4s$ for the odd parity and $3s^23p^2nd$ ($n = 3, 4$), $3s^23p^24s$, $3s3p^4$, $3s3p^34p$, $3s3p^34f$, $3s3p^23d^2$, $3s3p^23d4d$, $3s3p^23d4s$, $3s3p^24s^2$, $3p^4nd$ ($n = 3, 4$), $3p^44s$, $3p^33d4p$, $3p^33d4f$ for the even parity.

Correlation between the four valence electrons and the core subshells $1s^22s^22p^6$, which is not expected to affect considerably the oscillator strengths, was considered within the framework of a core-polarization potential and a correction to the dipole operator [48]. The estimate of these contributions requires the knowledge of the dipole polarizability of the ionic core, α_d, and of the cut-off radius, r_c. For the first parameter, we used the value computed by Johnson et al. [49] for K X, i.e. $\alpha_d = 0.03a_0^3$, while the cut-off radius, r_c, was chosen equal to $0.35a_0$ which corresponds to the HFR average value $\langle r \rangle$ of the outermost core orbital $2p^6$.

The semi-empirical optimization of the radial integrals was applied to all the experimentally known configurations, i.e. $3s^23p^3$, $3s^23p^23d$, $3s^23p^24s$ and $3s3p^4$, using the energy level values compiled by Sugar and Corliss [50]. The Slater parameters, not adjusted in this semi-empirical approach, were scaled down by 0.90 according to a well established procedure [47]. Due to space limitations, the parameters used and the details of the calculations are not reported here.

The HFR lifetime values calculated in K V, and reported only in the length form, are presented in Table 2.

2.2.2 The case of K VI

The configuration sets retained for intra-valence correlation were $3s^23p^2$, $3s^23pnp$ ($n = 4, 5$), $3s^23pnf$ ($n = 4, 5$), $3s3p^2nd$ ($n = 3$–5), $3s3p^2ns$ ($n = 4, 5$), $3s3p3dnp$ ($n = 4, 5$), $3s3p3dnf$ ($n = 4, 5$), $3p^4$, $3p^3np$ ($n = 4, 5$), $3p^3nf$ ($n = 4, 5$), $3p^23d^2$, $3p^23dnd$ ($n = 4, 5$), $3p^23dns$ ($n = 4, 5$) for the even parity and $3s^23pnd$ ($n = 3$–5), $3s^23pns$ ($n = 4, 5$), $3s3p^3$, $3s3p^2np$ ($n = 4, 5$), $3s3p^2nf$ ($n = 4, 5$), $3s3p3d^2$, $3s3p3dnd$ ($n = 4, 5$), $3s3p3dns$ ($n = 4, 5$), $3s3p4s^2$, $3p^3nd$ ($n = 3$–5), $3p^3ns$ ($n = 4, 5$), $3p^23dnp$ ($n = 4, 5$), $3p^23dnf$ ($n = 4, 5$) for the odd parity.

The effects of the $1s^22s^22p^6$ ionic core were estimated using the same parameters as in the case of K V.

Table 5. Oscillator strengths for transitions depopulating the $3s3p^2$, $3p^3$ and $3s3p3d$ levels in K VII. The table has been restricted to transitions with log $gf > -3.00$.

Transition[a]	λ^b (nm)	log gf^c
$3s3p^2\ {}^2D_{3/2} - 3s^23p\ {}^2P^\circ_{1/2}$	65.840	–0.83/–0.84
$-3s^23p\ {}^2P^\circ_{3/2}$	67.227	–1.71/–1.73
$3s3p^2\ {}^2D_{5/2} - 3s^23p\ {}^2P^\circ_{3/2}$	67.151	–0.61/–0.63
$3s3p^2\ {}^2S_{1/2} - 3s^23p\ {}^2P^\circ_{1/2}$	51.791	–0.61/–0.61
$-3s^23p\ {}^2P^\circ_{3/2}$	52.645	–0.62/–0.61
$3s3p^2\ {}^2P_{1/2} - 3s^23p\ {}^2P^\circ_{1/2}$	48.426	–0.14/–0.14
$-3s^23p\ {}^2P^\circ_{3/2}$	49.172	–0.32/–0.32
$3s3p^2\ {}^2P_{3/2} - 3s^23p\ {}^2P^\circ_{1/2}$	47.977	–0.38/–0.38
$-3s^23p\ {}^2P^\circ_{3/2}$	48.710	0.31/0.31
$3s^23d\ {}^2D_{3/2} - 3s^23p\ {}^2P^\circ_{1/2}$	39.894	0.23/0.24
$-3s^23p\ {}^2P^\circ_{3/2}$	40.399	–0.45/–0.44
$3s^23d\ {}^2D_{5/2} - 3s^23p\ {}^2P^\circ_{3/2}$	40.380	0.48/0.49
$3p^3\ {}^4S^\circ_{3/2} - 3s3p^2\ {}^4P_{1/2}$	51.779	–0.38/–0.38
$-3s3p^2\ {}^4P_{3/2}$	52.086	–0.08/–0.08
$-3s3p^2\ {}^4P_{5/2}$	52.561	0.09/0.09
$-3s3p^2\ {}^2P_{3/2}$	100.659	–2.94/–2.93
$3s3p3d\ {}^4P^\circ_{5/2} - 3s3p^2\ {}^4P_{3/2}$	40.534	0.07/0.09
$-3s3p^2\ {}^4P_{5/2}$	40.821	–0.15/–0.13
$-3s3p^2\ {}^2D_{5/2}$	47.519	–2.13/–2.12
$3s3p3d\ {}^4P^\circ_{3/2} - 3s3p^2\ {}^4P_{1/2}$	40.214	–0.03/–0.02
$-3s3p^2\ {}^4P_{3/2}$	40.398	–2.51/–2.50
$-3s3p^2\ {}^4P_{5/2}$	40.684	–0.45/–0.43
$-3s3p^2\ {}^2D_{3/2}$	47.295	–2.69/–2.68
$3s3p3d\ {}^4D^\circ_{1/2} - 3s3p^2\ {}^4P_{1/2}$	39.835	–0.18/–0.17
$-3s3p^2\ {}^4P_{3/2}$	40.016	–0.47/–0.45
$3s3p3d\ {}^4D^\circ_{3/2} - 3s3p^2\ {}^4P_{1/2}$	39.769	–0.37/–0.35
$-3s3p^2\ {}^4P_{3/2}$	39.950	0.10/0.12
$-3s3p^2\ {}^4P_{5/2}$	40.229	–0.55/–0.53
$-3s3p^2\ {}^2D_{3/2}$	46.682	–2.94/–2.93
$3s3p3d\ {}^4D^\circ_{5/2} - 3s3p^2\ {}^4P_{3/2}$	39.901	0.18/0.20
$-3s3p^2\ {}^4P_{5/2}$	40.179	0.17/0.19
$-3s3p^2\ {}^2D_{5/2}$	46.651	–2.51/–2.50
$3s3p3d\ {}^4D^\circ_{7/2} - 3s3p^2\ {}^4P_{5/2}$	40.155	0.61/0.63
$-3s3p^2\ {}^2D_{5/2}$	46.619	–2.47/–2.45

[a] Designation of the levels according to the NIST database [46]. The transitions are given in emission. [b] Calculated with the experimental energy levels given in the NIST database [46]. [c] Step 4 of the MCDF calculation (see the text). Corrected for the experimental wavelengths. Babushkin/Coulomb gauges.

A well-known semi-empirical fitting procedure of the calculated Hamiltonian eigenvalues to all the experimental energy levels compiled by Sugar and Corliss [50] was used allowing us to optimize all the radial integrals of the $3s^23p^2$, $3s^23p3d$, $3s^23p4s$ and $3s3p^3$ configurations. The Slater parameters not adjusted in this semi-empirical approach were scaled down by 0.90.

The HFR lifetime values for K VI are presented in Table 2 where they are compared with the MCDF results and with the only experimental result available for that ion.

2.2.3 The results for K VII

The configuration sets retained in this ion were $3s^2np$ ($n = 3$–6), $3s^2nf$ ($n = 4$–6), $3s3pnd$ ($n = 3$–6), $3s3pns$ ($n = 4$–6), $3s3dnp$ ($n = 4$–6), $3s3dnf$ ($n = 4$–6), $3p^3$, $3p^2np$ ($n = 4$–6), $3p^2nf$ ($n = 4$–6), $3p3d^2$, $3p3dnd$ ($n = 4$–6), $3p3dns$ ($n = 4$–6), $3d^24p$, $3d^24f$ for the odd parity and $3s^2nd$ ($n = 3$–6), $3s^2ns$ ($n = 4$–6), $3s3p^2$, $3s3pnp$ ($n = 4$–6), $3s3pnf$ ($n = 4$–6), $3s3d^2$, $3s3dnd$ ($n = 4$–6), $3s3dns$ ($n = 4$–6), $3s4s^2$, $3p^2nd$ ($n = 3$–6), $3p^2ns$ ($n = 4$–6), $3p3dnp$ ($n = 4$–6), $3p3dnf$ ($n = 4$–6), $3d^3$, $3d^24d$, $3d^24s$ for the even parity.

The core-polarization effects were estimated using the same approach as that described for K V and K VI.

The experimental energy levels compiled by Sugar and Corliss [50] were also retained to optimize some radial integrals of the $3s^23p$, $3s^24f$, $3s^25f$, $3s3p3d$, $3s3p4s$, $3p^3$ odd-parity and $3s^23d$, $3s^24d$, $3s^25d$, $3s^26d$, $3s^24s$, $3s^25s$, $3s^26s$, $3s3p^2$ even-parity configurations. As in K V and K VI, a scaling factor of 0.90 was also applied to the other Slater integrals.

The HFR lifetime values obtained for K VII are presented in Table 2.

The comparisons for the three ions (K V, K VI and K VII) show that the agreement between the MCDF and the HFR values is generally very satisfying. In fact, the ratio $\frac{|\tau_{HFR}-\tau_{MCDF(B)}|}{\tau_{MCDF(B)}}$ appears <0.10 for most transitions, the discrepancies between the two sets of results reaching 20% only for the $3s3p^3\ {}^3P^\circ_1$ and ${}^3D^\circ_1$ in K VI and for $3s3p^4\ {}^2P_{1/2,3/2}$ in K V. In the latter case, the origin of the discrepancy is probably due to the fact that it was not possible to include, in the MCDF calculations, the virtual excitations to the 5λ orbitals due to memory limitations (see the Sect. 2.1.1). Consequently, the MCDF results for the transitions originating from these two levels and reported in Table 3 could be less accurate.

As the MCDF results are generally considered as more accurate than the HFR data, they have been adopted for generating the results reported in Tables 3, 4 and 5.

3 Lifetime measurements

A further assessment of the MCDF results obtained in the present work can be established through comparisons with measurements of selected lifetimes.

Lifetime measurements in K V, K VI and K VII were carried out using the BFS method. A potassium beam of ∼0.2 μA was produced by the 2MV Van de Graaff accelerator of Liège University using the technique described in[51]. The principle of the method consisted in eroding by sputtering the exit channel of the radio frequency ion source after it has been covered with a thick coating of KCl. Xenon was chosen as buffer gas since its mass is very different from that of potassium. Very good discrimination could be obtained in the analysing magnet and a beam of pure K^+ ions could be sent through a thin home-made carbon foil (∼20 μg/cm^2) having a diameter of 6 mm. The light produced by the beam-foil interaction was observed at a right angle to the beam with a Seya-Namioka type spectrometer equipped with a 1 m radius 1200 l/mm concave grating. The grating is coated with Pt in order to improve reflectivity in the UV region. With this mounting, the efficiency of the grating was maximum around 60 nm.

The wavelength resolution (FWMH) was of the order of ∼0.12 nm (slits width 120 μm). The width of the part of the ion beam (diameter 5 mm) viewed by the spectrometer was 0.15 mm corresponding to a time resolution of 0.4 ns for a 1.7 MeV K beam. The light measurements were normalized to a fixed amount of charges entering the electrically isolated excitation chamber acting as a Faraday cup. The current was measured with a Ortec 439 current digitizer. The chamber was hold to a potential of +90V in order to reduce secondary electron loss through the chamber apertures.

For some earlier measurements, the light was detected by three Mullard (Philips) channeltron detectors aligned along the curved exit slit (width 120 μm) of the spectrometer. To measure the weak signal, a photon counting technique was used (the background was less than 1 cps). For the remaining decay curves, the exit slit was removed and replaced by a thin, back-illuminated, liquid nitrogen cooled CCD detector specially developed for far UV measurements. The CCD was tilted to an angle of 125° relatively to the spectrometer exit arm axis in order to be tangential to the Rowland circle. With this geometry, it had a dispersion of 0.02 nm/pixel and was able to detect light over a 20 nm wide region with a fairly constant resolution. The CCD detector system was supplied by the universities of Leicester and Lund. It is based on a EEV CCD15-11 chip of 27.6×6.9 mm (1040×280 of 27×27 μm square pixels) specially conditioned for UV light detection [52,53].

The CCD images were transferred to a networked computer and analyzed by a specially written software. The XY image was transformed by binning the horizontal lines into a file containing a list of numbers representing the light intensities as a function of the wavelength. The whole system was working under vacuum (10^{-5} Torr). The calibration of the spectra and the identification of the lines were based mainly on Kelly's tables [54] and the NIST web site [46].

For lifetime measurements, spectra have been recorded by moving the foil target upstream along the ion beam path. The measurements were made at beam energies of 1.7 MeV. At that energy, the charge state fraction of K V is ∼25%. The speed of the K ions after the foil has been calculated by taking into account the energy loss inside the foil [55]. A speed of of 2.9 mm/ns was used for the distance-to-time conversion.

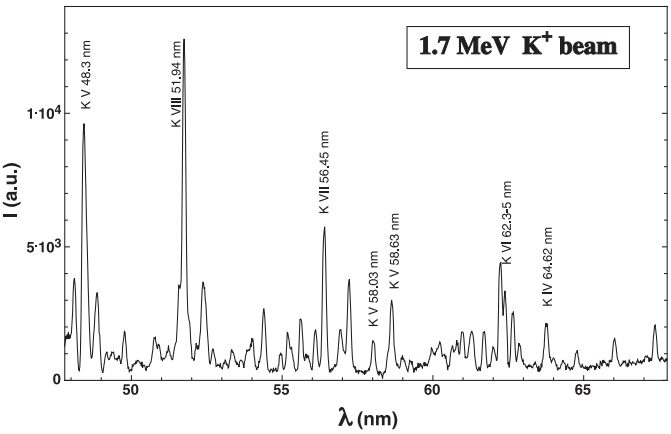

Fig. 2. BFS spectrum covering the region 45 to 70 nm. The light intensity, I (a.u.), is plotted vs. the wavelength, λ (nm).

The recording of the line intensity as a function of the foil holder position along the ion beam axis was fully automatized. The displacement of the foil was measured with a resolution of 10 μm by a digital gauge (Mitutoyo 5 MQ65-5P). At least 15 points were recorded for each curve and the stability of the foil position during the recording of each decay was checked. For data recorded with the CCD detector, the portion of the spectrum surrounding the line of interest was fitted with a Gaussian in order to subtract the background. The procedure was repeated for each position along the decay path and the amplitudes of the adjusted Gaussians were subsequently used for the decay analysis. The decay data were fitted with a model describing the whole decay curve as a growing part (close to the foil) followed by a multi-exponential decay in order to take into account the possible cascading process. The lifetime of the upper level of the transition has been deduced from the value of the decay constant of the main exponential contribution.

A part of the BFS spectrum covering the region 45 to 70 nm is reported in Figure 2. It has been recorded at an energy of 1.7 MeV. Some transitions of K V, K VI, K VII and K VIII are indicated on the figure.

A sample of a decay curve, as observed in the present work, is illustrated in Figure 3. It shows the intensity of the light as a function of the time (or the distance) after the foil.

The experimental lifetimes values obtained in this study are reported in Table 2. The quoted uncertainties represent twice the standard deviation of the mean. They are compared with previous measurements and with the calculations obtained in the present work (see above).

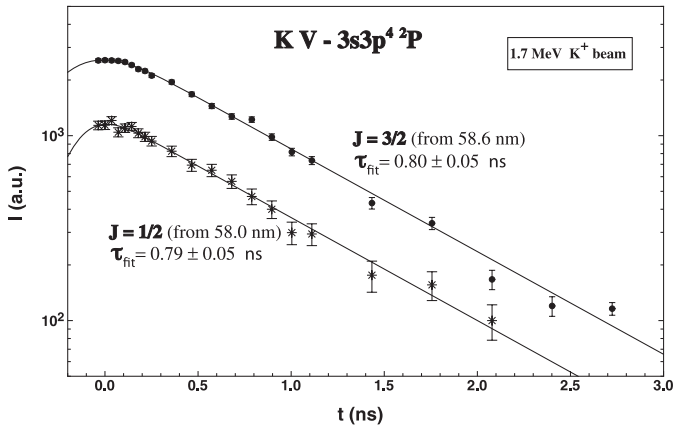

Fig. 3. Sample of a decay curve showing the intensity of the light, I (on a logarithmic scale), as a function of the time (or the distance) after the foil. The lifetime deduced from this K V decay curve is 0.75 ± 0.09 ns.

4 Discussion and conclusions

Cascade problems are frequently met in BFS lifetime measurements that use non-selective excitation and they generally lead to too long lifetimes. In fact, the decay curve involves a sum of many exponentials, one corresponding to the primary level and one to each level that cascades into it. While cascades that differ significantly in lifetime from that of the primary level do not pose a serious problem, cascades with lifetimes similar to that of the primary level can seriously distord a decay curve fit. Situations in which cascading is dominated by a few strong decay channels are ideally suited to the use of the adjusted normalization of decay curve (ANDC) technique [56,57]. In view of the very fragmentary knowledge of the energy level structure of the ions considered in the present paper, the use of the ANDC approach was not possible and, consequently, was not attempted here.

For K V, the MCDF(C) lifetimes agree with the BFS measurements within 13% for two levels, a larger discrepancy appearing for the level $3s3p^4\ ^2P_{1/2}$ level but this discrepancy has been explained above (see Sect. 2.2.3), the HFR lifetime agreeing however well with the measurement for this level. For the $3s3p^4\ ^2D_{5/2}$ level, the experimental result (characterized by a large uncertainty) is larger than the theoretical values.

In K VI, although the agreement theory-experiment is satisfying (within 30%), the measurement is longer than both the HFR and MCDF results (which agree) indicating that cascading problems could be eventually responsible of the discrepancy.

The agreement between theory (MCDF) and experiment in K VII is within 16% for the two $3s3p^2\ ^2D$ levels. The discrepancy found for the level $3s3p^2\ ^2D_{3/2}$ is probably due to a poor signal to noise ratio of the lines at 65.8 and 67.1 nm for which the intensity decay curves have been measured. The shorter lifetime measured for the level $3s3p^2\ ^2S_{1/2}$ is unexplained but the agreement for this level remains reasonable (40%).

The set of MCDF oscillator strengths presented in the present paper is concerning only strong transitions for which cancellation effects do not play a role in the calculations. The length and velocity results agree quite well in the MCDF scheme indicating that accurate wavefunctions have been used for the calculations. As the MCDF data agree generally well with the HFR results and also as the agreement between theoretical and experimental lifetimes values is satisfying in spite of the difficulties associated with the use of the BFS method in the specific case of the potassium ions (blending problems, difficulty to produce lines strong enough, possible cascading effects), they are expected to be accurate within a few percent (typically <10–20%) for most of the transitions.

Financial support from the Belgian Institut Interuniversitaire des Sciences Nucléaires (IISN) and from the FNRS is acknowledged. Three of us (É.B., P.P. and P.Q.) are respectively Research Director and Research Associates of this organization. Part of the work was carried out during the stay of one of us (E.B.) at Paris-Meudon Observatory. D. Rostohar has a postdoctoral grant of the FNRS. The cooperation of M. Clar during the acquisition of the data is gratefully acknowledged.

References

1. T. Andersen, A. Petrakiev Petkov, G. Sorensen, Phys. Scr. **12**, 283 (1975)
2. C.M. Varsavsky, Astrophys. J. Suppl. Ser. **53**, 75 (1961)
3. M.A. Ali, H.W. Joy, J. Phys. B **3**, 1552 (1970)
4. M. Aymar, Nucl. Instrum. Meth. **110**, 211 (1973)
5. P.S. Ganas, J. Opt. Soc. Am. **71**, 908 (1981)
6. K.-N. Huang, At. Data Nucl. Data Tables **30**, 313 (1984)
7. B.C. Fawcett, At. Data Nucl. Data Tables **35**, 203 (1986)
8. Y.K. Ho, R.J.W. Henry, Phys. Scr. **35**, 831 (1987)
9. E. Charro, I. Martin, M.A. Serna, J. Phys. B **33**, 1753 (2000)
10. C. Mendoza, C.J. Zeippen, Mon. Not. R. Astron. Soc. **198**, 127 (1982)
11. É. Biémont, J.E. Hansen, Phys. Scr. **31**, 509 (1985)
12. J.M. Malville, R.A. Berger, Planet. Space Sci. **13**, 1131 (1965)
13. P.F. Gruzdev, V.K. Prokof'ev, Opt. Spectrosc. **21**, 151 (1966)
14. M. Aymar, Physica **74**, 205 (1974)
15. P.S. Ganas, Physica C **111**, 365 (1981)
16. K.-N. Huang, At. Data Nucl. Data Tables **32**, 503 (1985)
17. É. Biémont, J. Opt. Soc. Am. B **3**, 163 (1986)
18. B.C. Fawcett, At. Data Nucl. Data Tables **36**, 129 (1987)
19. L.J. Curtis, Phys. Rev. A **40**, 6958 (1989)
20. E. Charro, I. Martin, C. Lavin, Astron. Astrophys. Suppl. Ser. **124**, 397 (1997)
21. C. Mendoza, C.J. Zeippen, Mon. Not. R. Astron. Soc. **199**, 1025 (1982)
22. É. Biémont, G.E. Bromage, Mon. Not. R. Astron. Soc. **205**, 1085 (1983)
23. L. Engström, M. Kirm, P. Bengtsson, S.T. Maniak, L.J. Curtis, E. Träbert, J. Doerfert, J. Granzow, Phys. Scr. **52**, 516 (1995)
24. C.F. Fischer, J. Quant. Spectrosc. Radiat. Transfer **8**, 755 (1968)

25. C.F. Fischer, Can. J. Phys. **54**, 740 (1976)
26. C.F. Fischer, Can. J. Phys. **56**, 983 (1978)
27. R. Mewe, Astron. Astrophys. **59**, 275 (1977)
28. A. Farrag, E. Luc-Koenig, J. Sinzelle, J. Phys. B **14**, 3325 (1981)
29. K. Aashamar, T.M. Luke, J.D. Talman, Phys. Scr. **30**, 121 (1984)
30. K.-N. Huang, At. Data Nucl. Data Tables **34**, 1 (1986)
31. J.F. Thornbury, A. Hibbert, E. Träbert, Phys. Scr. **40**, 472 (1989)
32. M. Hjorth-Jensen, K. Aashamar, Phys. Scr. **42**, 309 (1990)
33. S.-S. Liaw, Can. J. Phys. **70**, 644 (1992)
34. R. Marcinek, J. Migdalek, J. Phys. B **26**, 1391 (1993)
35. C. Lavin, A.B. Alvarez, I. Martin, J. Quant. Spectrosc. Radiat. Transfer **57**, 831 (1997)
36. B. Warner, Z. Astrophys. **69**, 399 (1968)
37. É. Biémont, J.E. Hansen, Phys. Scr. **34**, 116 (1986)
38. F.A. Parpia, C. Froese Fischer, I.P. Grant, Comp. Phys. Commun. **94**, 249 (1996)
39. I.P. Grant, Meth. Comp. Chem. **2**, 1 (1988)
40. B.J. McKenzie, I.P. Grant, P.H. Norrington, Comp. Phys. Commun. **21**, 233 (1980)
41. I.P. Grant, B.J. McKenzie, P.H. Norrington, D.F. Mayers, N.C. Pyper, Comp. Phys. Commun. **21**, 207 (1980)
42. T. Brage, D.S. Leckrone, C. Froese Fischer, Phys. Rev. A **53**, 192 (1996)
43. T. Brage, C. Proffitt, D.S. Leckrone, Astrophys. J. **513**, 524 (1999)
44. É. Biémont, C. Froese Fischer, M.R. Godefroid, P. Palmeri, P. Quinet, Phys. Rev. A **62**, 032512 (2000)
45. P. Palmeri, P. Quinet, É. Biémont, Phys. Scr. **63**, 468 (2001)
46. `http://physics.nist.gov/cgi-bin/AtData/main_asd`
47. R.D. Cowan, *Theory of Atomic Structure and Spectra* (University of California Press, Berkeley, 1981)
48. P. Quinet, P. Palmeri, É. Biémont, M.M. McCurdy, G. Rieger, E.H. Pinnington, J.E. Lawler, M.E. Wickliffe, Mon. Not. R. Astr. Soc. **307**, 934 (1999)
49. W.R. Johnson, D. Kolb, K.-N. Huang, At. Data Nucl. Data Tables **28**, 333 (1983)
50. J. Sugar, C. Corliss, J. Phys. Chem. Ref. Data **14** (1985)
51. X. Tordoir, H.P. Garnir, P.-D. Dumont, Nucl. Instrum. Meth. B **140**, 251 (1998)
52. R. Hutton, Y. Zou, S. Huldt, I. Martinson, K. Ando, B. Nyström, T. Kambara, H. Oyama, Y. Awaya, Phys. Scr. **T80**, 552 (1999)
53. H.-P. Garnir, P.-H. Lefèbvre, Nucl. Instrum. Meth. B **235**, 530 (2005)
54. R.L. Kelly, J. Phys. Chem. Ref. Data **16** (1987)
55. F.S. Garnir-Monjoie, Y. Baudinet-Robinet, H.P. Garnir, P.D. Dumont, J. Phys. France **40**, 41 (1980)
56. L.J. Curtis, J. Bromander, H.G. Berry, Phys. Lett. A **34**, 169 (1971)
57. L.J. Curtis, *Atomic Structure and Lifetimes, A Conceptual Approach* (Cambridge University Press, Cambridge, 2003)